

A Deep Learning Model for Improved Wind and Wave Forecasts

Yuval Yevnin¹, Yaron Toledo¹

¹School of Mechanical Engineering, Tel-Aviv University, Tel-Aviv 69978, Israel

Key Points:

- A deep learning recurrent-convolution model improves wind forecast. The wind prediction is used as input for the wave forecasting model.
- The model improves wind and wave forecasts RMSE by $\sim 10\%$ over the Mediterranean, and $\sim 35\%$ over the Aegean Sea during the Etesian winds.
- The model has negligible additional computational costs, and can be generalized to a global grid or specialized to a local grid.

Corresponding author: Yuval Yevnin, yuval.yevnin@gmail.com

Corresponding author: Yaron Toledo, toledo@tau.ac.il

Abstract

The paper presents a combined numerical - deep learning (DL) approach for improving wind and wave forecasting. First, a DL model is trained to improve wind velocity forecasts by using past reanalysis data. The improved wind forecasts are used as forcing in a numerical wave forecasting model. This novel approach, used to combine physics-based and data-driven models, was tested over the Mediterranean. It resulted in $\sim 10\%$ RMSE improvement in both wind velocity and wave height forecasts over operational models. This significant improvement is even more substantial at the Aegean Sea from May to September, when Etesian winds are dominant, improving wave height forecasts by over 35%. The additional computational costs of the DL model are negligible compared to the costs of either numerical models. This work has the potential to greatly improve the wind and wave forecasting models used nowadays by tailoring models to localized seasonal conditions, at negligible additional computational costs.

Plain Language Summary

Modern wave forecasting originated in the D-Day invasion, while attempting to predict the optimal date for departure. In the decades since, it has advanced and currently forecasting models are sets of complicated, physics-based equations. Similar, and even more complex models are used to make wind forecasts which are needed as inputs for the wave models. This work presents a deep learning model improving the wind forecast, and consequently improving also the wave forecast. The novel approach of combining deep learning and classical forecasting models was tested over the Mediterranean Sea, and resulted in $\sim 10\%$ improvement in both wind and wave forecasts over the current operational model. This significant improvement is even more substantial when examining the local region of the Aegean Sea during May to September, when the Etesian wind is dominant, improving wave height forecasts by over 35%. This work has the potential to revolutionize the weather forecasting models used nowadays by tailoring models to localized seasonal conditions, with negligible additional computational costs. The derived methodology can also be applied to various other fields, where the deep learning model can learn to predict measured or simulated results from an initial, less accurate model.

1 Introduction

Wind velocity accuracy has been established as one of the most significant factors in achieving an accurate ocean waves forecast (Bidlot et al., 2002). For this reason, operational wave forecasting models aim to use the most accurate wind fields available, with a high resolution in both space and time. The models producing these wind fields are highly computationally expansive, simulating many layers in the atmosphere. These atmospheric models are assimilated with data acquired by measurement instruments to create reanalysis results. The reanalysis data is used to assess, study and improve the forecast ability (Hersbach et al., 2020).

Traditionally, wave forecasting models, such as WAM (Hasselmann et al., 1988), WAVEWATCH III (Tolman, 1991) or SWAN (Booij et al., 1999), use wind forecast as an input. Although the driving force for wave generation is surface wind, the parameter used by most models is wind velocity at $10m$ above the sea surface (U10), as this property is easier to measure and predict. This means only a single property at a single level of the atmospheric model actually affects the wave model. A semi-empirical source term is used by wave models to convert U10 to wave action forcing (Janssen & Janssen, 2004; Ardhuin et al., 2010). Optimizing atmospheric models is highly complex, both in terms of computational costs and in terms of improved physical equations accounting for multiple flow parameters. Thus, a model which can optimize U10 independently, decoupled from the physics-based model and with low computational costs, is very desirable.

In the last few years, deep learning (DL) models have been used in multiple fields to solve complex, highly nonlinear problems (Wang et al., 2019; Brunton et al., 2020). These DL models are data-driven, meaning they generally do not possess any prior physical knowledge, but are instead trained to predict a given “ground-truth” data. After the model is trained using a training dataset to achieve good performance, it is verified over an independent test dataset. The training process usually requires more significant computational resources, though it is still relatively small compared to numerical models. Afterwards, the resulting model can be used to produce accurate predictions at very minimal computational cost.

DL methods are highly relevant for geophysical problems (Reichstein et al., 2019), and can be used for various functions. First, DL is used for making forecasts directly, which are data-driven and independent of physical equations and numerical models (Scher & Messori, 2019; Weyn et al., 2019, 2020; Rasp & Thuerey, 2020; Rasp et al., 2020; Arcomano et al., 2020). Second, these are used in hybrid numerical-DL models, where the DL model usually replaces some functions or parameterization of the numerical model in order to increase computational efficiency (Krasnopolsky et al., 2005; Krasnopolsky & Fox-Rabinovitz, 2006; Krasnopolsky et al., 2010; Schneider et al., 2017; Gentine et al., 2018; Rasp et al., 2018; Pathak et al., n.d.; “Prognostic Validation of a Neural Network Unified Physics Parameterization”, 2018; Brenowitz & Bretherton, 2019; Wikner et al., 2020). Finally, machine learning (ML) and DL methods are used for post-processing and measurement assimilation (Vannitsem et al., 2020; Haupt et al., 2021). These usually use an ensemble as an input to a ML model based on random forest or a fully-connected neural network (NN) (Zjavka, 2015; Rasp & Lerch, 2018), while recently some work has been done using convolutional NN (Grönquist et al., 2020; Veldkamp et al., 2020).

The presented paper uses a DL model with U10 wind velocity forecasts as the input, and predicts the reanalysis data, considered as “ground-truth”. This is a form of post-processing, and is intended to improve wind prediction used as an input to a numerical wave model. Unlike previous works, the current model focuses on using advanced DL architecture to improve forecasts using only the predicted variable as input. This allows the DL model to be used in wave forecasting as a wind pre-process source term. To the best of our knowledge, this is the first attempt to create such an integrated numerical - deep learning process to improve wind forecasting in view of operational wave forecasting needs.

2 Model Database - ECMWF Wind Velocity

The datasets used in this paper are ECMWF ERA5 reanalysis (REAN) and the forecasts (FC) which were used as initial model for the reanalysis (Hersbach et al., 2020). ERA5 was chosen as it was found to be a very accurate reanalysis for surface winds (Ramon et al., 2019). The parameters of wind velocity in the zonal and meridional directions at 10m height (u_{10}, v_{10}) were used, where FC data was used as the DLM input and the REAN as the “ground-truth”.

The FC is initiated from a wind analysis every 12 hours at 06:00 and 18:00, and consists of 18 hourly steps. This means there is an overlap between consecutive forecasts. In this work the time steps 7-18 were chosen, as these were furthest from the initial analysis and had the largest errors. The REAN data is an hourly high-resolution model incorporated with measurements.

The spatial grid chosen was of the Mediterranean region, with longitude between $30.2-45.7N$ and steps of $0.5N$, and latitude between $-2.1-36.0E$ and steps of $0.3E$. This results in a base 2 grid of dimensions 32×128 , making it efficient for processing with a DLM.

111

3 Recurrent-Convolutional Model

112

113

114

115

116

117

118

119

120

121

In Roitenberg and Wolf (2019) a general DLM architecture for spatio-temporal forecasting problems was introduced and tested for public transportation demand. This model was used as a base for a new DLM, by removing the encoder and making several adjustments to the decoder part (Fig. 1). The new DLM begins with an input sequence of FC instances. Next is an encoder comprised of convolutional layers with gradually increasing width and dilation. Increasing the width allows each layer to capture more information, while larger dilation allows a wider receptive field, taking into account the effects of further spatial information. Using dilation instead of more traditional approaches of strided convolution or pooling layers keeps the original input dimensions, and thus prevents spatial information loss (Yu & Koltun, 2015).

122

123

124

125

126

127

128

129

130

131

132

Following the encoder, Convolutional Gated Recurrent Unit (CGRU) (Ballas et al., 2015) layers were used. These layers combine the ability of the GRU layer (Chung et al., 2014) to learn temporal connections with the convolutional layer capability of spatial modelling. This is done by replacing the matrix multiplication of a GRU with a convolution, and the parameter matrices and vectors with smaller kernels. Each instance of the input sequence is introduced separately to the encoder and to the following CGRU, and the last output of the CGRU is concatenated with the last input instance into it. This forms a skip connection over the CGRU, allowing both to bypass it where needed, and to improve it by adding a residual. Using residual connections was shown to be extremely effective in improving the learning ability of the neural networks compared to modelling absolute values (Littwin & Wolf, 2016).

133

134

135

Finally, the new decoder consists of convolution layers mirroring the structure of the encoder in width and dilation. The output of the decoder was summed with the last input instance to the model, forming another residual connection.

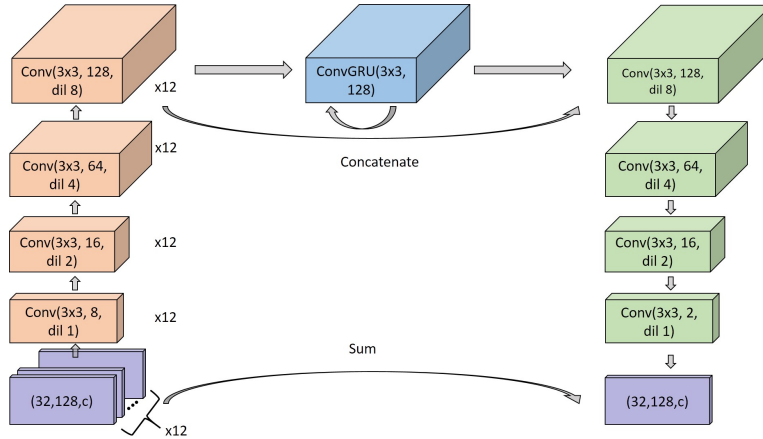


Figure 1. Model architecture from bottom left: input (purple) in the form of a sequence of FC instances with c channels (variables) is passed one at a time to the encoder (orange), comprised of convolutional layers with increasing filters and dilation. The output of the encoder is fed to a CGRU (blue). The last output of the resulting sequence is concatenated with the last input into it, and introduced to the decoder (green), comprised of convolutional layers mirroring the encoder. The final result is summed with the last instance of the input sequence to form a residual connection (purple).

Table 1. *Wind velocity RMSE*

Model	Property	DLM RMSE	FC RMSE	RMSE improved
UMag, sec. 4.1	$U[m/s]$	0.5999	0.6673	10.1%
	$u_{10}[m/s]$	0.7075	0.7291	2.97%
	$v_{10}[m/s]$	0.7065	0.7278	2.88%
UVec, sec. 4.2	$U[m/s]$	0.615	0.6673	7.8%
	$u_{10}[m/s]$	0.6616	0.7291	9.26%
	$v_{10}[m/s]$	0.6594	0.7278	9.39%
UDir, sec. 4.3	$\cos \theta$	0.2307	0.2469	6.55%
	$\sin \theta$	0.229	0.2463	7.04%
	$u_{10}[m/s]$	0.6906	0.7291	5.28%
	$v_{10}[m/s]$	0.69	0.7278	5.19%
UFrc, sec. 4.4	$U[m/s]$	0.6162	0.6673	7.65%
	$u_{10}[m/s]$	0.663	0.7291	9.06%
	$v_{10}[m/s]$	0.6613	0.7278	9.14%

4 Deep Learning Wind Prediction Experiments

Four types of wind input to the DLM were tested for effectiveness in producing a more accurate wind input for wave forecasting. The input data for all experiments consisted of 12 consecutive hourly time steps from the FC dataset. The target was the REAN at the time of the last input. This effectively means improving the wind field at a given time t by using time steps $(t-11, t)$. The network hyper-parameters were initially set to those of Roitenberg and Wolf (2019). A short training period of the years 2010–2011 and validation period of the year 2012 was used to test changes to the architecture. Due to long run times even for these short periods, an extensive architectural grid search was not conducted. The chosen architecture (shown in Fig. 1) consisted of a four convolutional layers encoder with (8, 16, 64, 128) filters and a dilation of (1, 2, 4, 8), followed by a single CGRU layer with input and output dimensions of 128. The decoder consisted of four convolutional layers with (128, 32, 16, 2) filters and (8, 3, 2, 1) dilations. The datasets were split into a training set between the years 2001–2016, a validation set of the year 2000 and a test set of the year 2017. The validation set was used for hyperparameter tuning and internal model verification. It was separated from the test set to prevent similarities between the two. The presented results refer only to the test set. The DLM was trained and evaluated using an NVidia GeForce GTX 2080 Ti GPU with a 12GB memory. The Fastai API (Howard & Gugger, 2020) was used with Pytorch API as a base. The model was optimized using ADAM (Kingma & Ba, 2015). Weight decay was set to $1E-3$, and the mini-batch size was 16. A changing learning rate with the 1-cycle approach of (Smith, 2018) was used, and each model was trained for 8 cycles of 2 epochs. The max learning rate started at $1E-3$, and was divided by the cycle number as learning progressed. After training, the validation set was used to identify the cycle with best performance. The weights of this cycle defined the new DLM, and its performance was evaluated on the test set. The resulting RMSE in space and time of all wind input types are shown in Table 1 and compared to the original FC data. Additional statistics and figures are available in the supporting information.

165 4.1 Input type 1: Wind Velocity Magnitude

166 The first experiment optimized prediction of wind velocity magnitude (UMag), de-
 167 fined as $U = \sqrt{u_{10}^2 + v_{10}^2}$. The magnitude was chosen as it seemed easier to predict, be-
 168 ing always positive, non-directional and independent property in space. This resulted
 169 with input and output tensors with dimensions of ($time = 12, c = 1, lat = 32, lon =$
 170 128). The resulting U was also transformed back to the form of u_{10} and v_{10} using the
 171 original FC direction. As expected, U improved significantly, as it is the main objective
 172 of the UMag DLM. It is interesting that the resulting u_{10} and v_{10} are improved by a
 173 much smaller percentage.

174 4.2 Input type 2: Wind Velocity Vector

175 The second experiment was performed to test the DLM's ability to improve the wind
 176 velocity vector (UVec) directly. The input was set as the FC u_{10} and v_{10} , and the out-
 177 put as the matching prediction, resulting with (12, 2, 32, 128) tensors. Although the im-
 178 provement in the main objective of each DLM is smaller, the resulting wind vector im-
 179 provement is almost three times as much as that of the UMag model.

180 4.3 Input type 3: Wind Direction Vector

181 The third experiment was predicting the direction of the wind velocity vector (UDir).
 182 The normalized directional vector (unit vector) was defined as

$$\begin{pmatrix} \cos \theta \\ \sin \theta \end{pmatrix} = \begin{pmatrix} u_{10}/U \\ v_{10}/U \end{pmatrix}, \quad (1)$$

183 and was set as both the input and output of the DLM. The test set output was multi-
 184 plied by U to produce a wind velocity vector. Examining the results of this DLM found
 185 it similar to the UVec model with smaller improvement.

186 4.4 Input type 4: Wind Friction Velocity Vector

187 Finally, an experiment was carried out to try and make a connection between a phys-
 188 ical wave forecasting model and the DLM for wind prediction. The wave model uses the
 189 wind input through a source term (ST) which converts it to wave energy. Such a ST com-
 190 bines analytical and empirical derivations, with a varying degree of complexity. The re-
 191 latively simple wind friction velocity vector (UFrc) of WAM 3 (WAMDI Group, 1988)

$$\mathbf{u}_* = \begin{pmatrix} u_{10}\sqrt{0.8 + 0.065u_{10}} \\ v_{10}\sqrt{0.8 + 0.065v_{10}} \end{pmatrix}, \quad (2)$$

192 was used in the DLM cost function. which should make it better fitting as an input to
 193 the ST. This still lacks the local wave action spectrum used in the source term, but as
 194 they are the result of an independent model with high computational cost, such a cou-
 195 pled model was not tested. This DLM's results were almost identical to the UVec model.

196 5 Wave forecasting with deep learning wind prediction

197 The effects of the new DLM output (the wind velocity prediction) on ocean waves
 198 forecasting was examined by using it as a forcing of the WAVEWATCH III v6.07 (WW3)
 199 model. WW3 ran with an unstructured grid of the eastern (Levant) area of the Mediter-
 200 ranean Sea, using 36 directions, 36 frequencies in the range 0.04–0.427Hz and a time
 201 step of $dt_{global} = 10min$. The wind forcing source term of Ardhuin et al. (2010) was
 202 used, alongside a linear wind interpolation. Six input configurations were tested: ECMWFs
 203 FC and REAN, and the four DLM outputs. WW3 ran separately with each forcing for
 204 the year 2017. The resulting wave forecast mean field parameters of significant wave height

Table 2. *Model wave mean parameters RMSE*

Property	FC	UMag (%improved)	UVec (%)	UDir (%)	UFrc (%)
$H_s[m]$	0.0765	0.0676 (11.6%)	0.0698 (8.7%)	0.0762 (0.4%)	0.0705 (7.8%)
$Dir[deg]$	44.4	42.8 (3.4%)	42.2 (4.9%)	43.8 (1.3%)	42.5 (4.3%)
$T_{m0,-1}[sec]$	0.309	0.283 (8.4%)	0.286 (7.4%)	0.307 (0.05%)	0.287 (7.1%)

(H_s), mean wave direction (dir) and mean wave period ($T_{m0,-1}$) are shown in Table 2. All DLM outperformed the FC, as expected. Surprisingly, UMag had the best performance for both wave height and period, while UVec results with a better mean direction. UDir was outperformed by the other models and UFrc was almost identical to UVec with slightly worse results. Thus, only UMag and UVec are shown in the following analysis.

211

A spatial map of H_s time-mean RMSE differences can be seen in Fig. 2. The RMSE difference was taken as $RMSE_{FC} - RMSE_{DLM}$, meaning the new DLM has better performance where positive and vice versa. It is immediately apparent that both DLM outperform the original FC in the eastern part of the basin, especially in the Aegean Sea where the local improvement is $\sim 20\%$. The FC slightly outperforms the DLM at the southwestern part. This spatial difference is correlated to a much higher RMSE in the original FC data at the eastern half, specifically in the Aegean Sea (see Fig. S8). The large RMSE results in larger gradients while training the DLM, and thus greater improvement. The improved performance of UMag can be attributed to more accurate results over the western half, including improved performance along the coastal area. This spatial deviation suggests that applying a mask during the training process or combining the prediction with FC might be beneficial.

A temporal comparison of spatial-mean RMSE of the DLM and FC is given in Fig. 3. This shows that the main improvement of both DLM was during the spring to autumn period, most prominently during the summer months (implying correction of the Etesian wind). Examining the Aegean Sea during the Etesian results in a staggering 35% RMSE improvement. The current model can be used as is, or as a seasonal model, alongside a separate seasonal model trained specifically for the winter season or even for stormy conditions. Such models can work as an ensemble to produce better results.

6 Summary and discussion

In this work a novel deep learning model for wind velocity post-processing was presented. The model allows to improve wind and waves numerical, physics-based models' accuracy by using a deep learning, data-driven model (DLM). The DLM's input were the forecasts (FC) which were used in ECMWF ERA5 reanalysis (REAN), and the "ground-truth" was the REAN data itself. This model consisted of a convolutional encoder and decoder, with a convolutional gated recurrent unit in between. The DLM's output was used as a forcing for a wave forecasting model (WAVEWATCH III), and the resulting significant wave height, mean wave direction and mean wave period were examined. The new model showed significant improvement in all wind and wave parameters.

The presented DLM was used to improve wind velocity, but could easily be trained to improve any other parameter of the atmospheric model, such as geopotential height

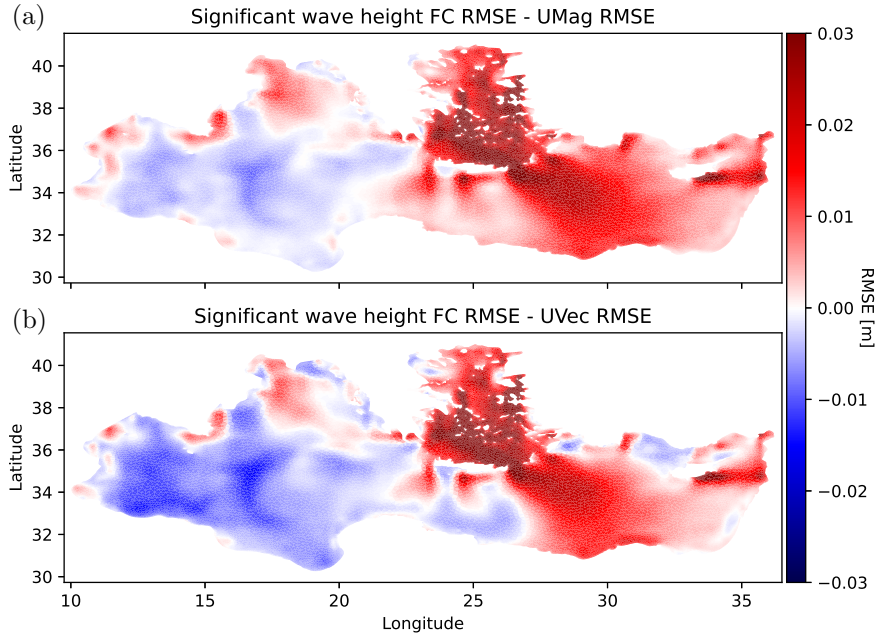


Figure 2. Time-mean RMSE difference map of significant wave height H_s for: (a) FC RMSE - UMag RMSE; (b) FC RMSE - UVec RMSE. FC with larger error in red, DLM in blue.

243 or temperature. It could also be trained over different locations, or as a global model.
 244 Furthermore, another very interesting usage is training towards seasonal localized mod-
 245 els. These could be optimized over specific time periods and locations where weather con-
 246 ditions are hard to predict, and result in significant improvement. One such example is
 247 shown in this work at the Aegean Sea, where the Etesian wind is dominant during mid-
 248 May to mid-September. Even without training specifically for this task, the presented
 249 model improves the significant wave height forecast over the Aegean Sea at this period
 250 by $\sim 35\%$.

251 Another benefit of the new model is very minimal computational cost, which is neg-
 252 ligible when compared to either the numerical wind or wave forecasting models. Further-
 253 more, it could easily be implemented, as it does not require any adjustment to any of
 254 the currently used operational models, while providing significant improvement in fore-
 255 casting results.

256 Acknowledgments

257 This research was supported by: the ISRAEL SCIENCE FOUNDATION [grant No. 1601/20]
 258 and The Gordon Center for Energy Studies. The authors would like to thank Prof. Lior
 259 Wolf for his insights and helpful discussion.

260 Author Contribution

261 Y.Y. conceived the research, created the deep learning model and performed the
 262 experiments. Y.T. supervised the work. Both authors wrote the manuscript

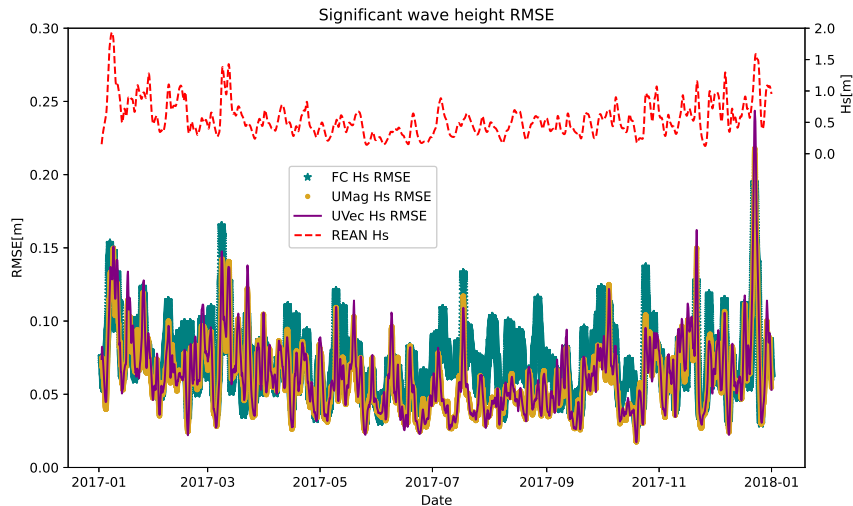


Figure 3. Spatial-mean RMSE of significant wave height H_s 24hrs moving average of: FC (thick teal); UMag (medium orange); UVec (thin purple). The right axis is the REAN H_s in dashed red line, for reference.

263 Data Availability

264 The code to recreate the work is available at: <https://doi.org/10.5281/zenodo.5016491/>
 265 . The ERA5 wind data is available from ECMWF and the Copernicus Climate Data Store
 266 database at <https://cds.climate.copernicus.eu/> . The WAVEWATCH III wave model is
 267 available at <https://polar.ncep.noaa.gov/waves/> .

268 References

- 269 Arcomano, T., Szunyogh, I., Pathak, J., Wikner, A., Hunt, B. R., & Ott, E. (2020,
 270 may). A Machine Learning-Based Global Atmospheric Forecast Model. *Geo-*
 271 *physical Research Letters*, *47*(9).
- 272 Ardhuin, F., Rogers, E., Babanin, A. V., Filipot, J.-F., Magne, R., Roland, A., ...
 273 Collard, F. (2010). Semiempirical Dissipation Source Functions for Ocean
 274 Waves. Part I: Definition, Calibration, and Validation. *Journal of Physical*
 275 *Oceanography*, *40*(9), 1917–1941.
- 276 Ballas, N., Yao, L., Pal, C., & Courville, A. (2015, nov). Delving Deeper into Con-
 277 volutional Networks for Learning Video Representations. *4th International*
 278 *Conference on Learning Representations, ICLR 2016 - Conference Track Pro-*
 279 *ceedings*.
- 280 Bidlot, J. R., Holmes, D. J., Wittmann, P. A., Lalbeharry, R., & Chen, H. S. (2002,
 281 apr). Intercomparison of the performance of operational ocean wave forecasting
 282 systems with buoy data. *Weather and Forecasting*, *17*(2), 287–310.
- 283 Booij, N., Ris, R. C., & Holthuijsen, L. H. (1999, apr). A third-generation wave
 284 model for coastal regions. 1. Model description and validation. *J. Geophys.*
 285 *Res.*, *104*(C4).
- 286 Brenowitz, N. D., & Bretherton, C. S. (2019, aug). Spatially Extended Tests of a
 287 Neural Network Parametrization Trained by Coarse-Graining. *Journal of Ad-*
 288 *vances in Modeling Earth Systems*, *11*(8), 2728–2744.
- 289 Brunton, S. L., Noack, B. R., & Koumoutsakos, P. (2020, jan). Machine Learning for

- 290 Fluid Mechanics. *Annual Review of Fluid Mechanics*, 52(1), 477–508.
- 291 Chung, J., Gulcehre, C., Cho, K., & Bengio, Y. (2014, dec). Empirical Evaluation of
292 Gated Recurrent Neural Networks on Sequence Modeling.
- 293 Gentine, P., Pritchard, M., Rasp, S., Reinaudi, G., & Yacalis, G. (2018, jun). Could
294 Machine Learning Break the Convection Parameterization Deadlock? *Geophys-*
295 *ical Research Letters*, 45(11), 5742–5751.
- 296 Grönquist, P., Yao, C., Ben-Nun, T., Dryden, N., Dueben, P., Li, S., & Hoefler, T.
297 (2020, may). Deep Learning for Post-Processing Ensemble Weather Forecasts.
298 *Philosophical Transactions of the Royal Society A: Mathematical, Physical and*
299 *Engineering Sciences*, 379(2194).
- 300 Hasselmann, K., Hasselmann, S., Bauer, E., Janssen, P. A., Komen, G. J., Bertotti,
301 L., ... Ewing, J. A. (1988, dec). *The WAM model - a third generation ocean*
302 *wave prediction model*. (Vol. 18; Tech. Rep. Nos. 12, Dec. 1988).
- 303 Haupt, S. E., Chapman, W., Adams, S. V., Kirkwood, C., Hosking, J. S., Robinson,
304 N. H., ... Subramanian, A. C. (2021, apr). *Towards implementing artificial*
305 *intelligence post-processing in weather and climate: Proposed actions from the*
306 *Oxford 2019 workshop* (Vol. 379) (No. 2194). Royal Society Publishing.
- 307 Hersbach, H., Bell, B., Berrisford, P., Hirahara, S., Horányi, A., Muñoz-Sabater, J.,
308 ... Thépaut, J. N. (2020, jul). The ERA5 global reanalysis. *Quarterly Journal*
309 *of the Royal Meteorological Society*, 146(730), 1999–2049.
- 310 Howard, J., & Gugger, S. (2020, feb). fastai: A Layered API for Deep Learning. *In-*
311 *formation (Switzerland)*, 11(2).
- 312 Janssen, P., & Janssen, P. A. E. M. (2004). *The interaction of ocean waves and*
313 *wind*. Cambridge University Press.
- 314 Kingma, D. P., & Ba, J. L. (2015, dec). Adam: A method for stochastic optimiza-
315 tion. In *3rd international conference on learning representations, iclr 2015 -*
316 *conference track proceedings*. International Conference on Learning Representa-
317 tions, ICLR.
- 318 Krasnopolsky, V. M., & Fox-Rabinovitz, M. S. (2006, mar). Complex hybrid mod-
319 els combining deterministic and machine learning components for numerical
320 climate modeling and weather prediction. *Neural Networks*, 19(2), 122–134.
- 321 Krasnopolsky, V. M., Fox-Rabinovitz, M. S., & Belochitski, A. A. (2010). Devel-
322 opment of neural network convection parameterizations for numerical climate
323 and weather prediction models using cloud resolving model simulations. In
324 *Proceedings of the international joint conference on neural networks*.
- 325 Krasnopolsky, V. M., Fox-Rabinovitz, M. S., & Chalikov, D. V. (2005, may). New
326 approach to calculation of atmospheric model physics: Accurate and fast neu-
327 ral network emulation of longwave radiation in a climate model. *Monthly*
328 *Weather Review*, 133(5), 1370–1383.
- 329 Littwin, E., & Wolf, L. (2016, nov). The Loss Surface of Residual Networks: Ensem-
330 bles and the Role of Batch Normalization.
- 331 Pathak, J., Wikner, A., Fussell, R., Chandra, S., Hunt, B. R., Girvan, M., & Ott, E.
332 (n.d.). *Hybrid Forecasting of Chaotic Processes: Using Machine Learning in*
333 *Conjunction with a Knowledge-Based Model* (Tech. Rep.).
- 334 Prognostic Validation of a Neural Network Unified Physics Parameterization. (2018,
335 jun). *Geophysical Research Letters*, 45(12), 6289–6298.
- 336 Ramon, J., Lledó, L., Torralba, V., Soret, A., & Doblas-Reyes, F. J. (2019, oct).
337 What global reanalysis best represents near-surface winds? *Quarterly Journal*
338 *of the Royal Meteorological Society*, 145(724), 3236–3251.
- 339 Rasp, S., Dueben, P. D., Scher, S., Weyn, J. A., Mouatadid, S., & Thuerey, N.
340 (2020, feb). Weatherbench: A benchmark dataset for data-driven weather
341 forecasting.
- 342 Rasp, S., & Lerch, S. (2018, nov). Neural networks for postprocessing ensemble
343 weather forecasts. *Monthly Weather Review*, 146(11), 3885–3900.

- 344 Rasp, S., Pritchard, M. S., & Gentine, P. (2018). Deep learning to represent subgrid
345 processes in climate models.
- 346 Rasp, S., & Thuerey, N. (2020, aug). Data-driven medium-range weather prediction
347 with a Resnet pretrained on climate simulations: A new model for Weather-
348 Bench.
- 349 Reichstein, M., Camps-Valls, G., Stevens, B., Jung, M., Denzler, J., Carvalhais, N.,
350 et al. (2019). Deep learning and process understanding for data-driven earth
351 system science. *Nature*, *566*(7743), 195–204.
- 352 Roitenberg, A., & Wolf, L. (2019). Forecasting traffic with a convolutional gru de-
353 coder conditioned on adapted historical data. *ICML 2019 Time Series Work-*
354 *shop*.
- 355 Scher, S., & Messori, G. (2019, jul). Weather and climate forecasting with neural
356 networks: Using general circulation models (GCMs) with different complexity
357 as a study ground. *Geoscientific Model Development*, *12*(7), 2797–2809.
- 358 Schneider, T., Lan, S., Stuart, A., & Teixeira, J. (2017, dec). Earth System Model-
359 ing 2.0: A Blueprint for Models That Learn From Observations and Targeted
360 High-Resolution Simulations. *Geophysical Research Letters*, *44*(24), 12,396–
361 12,417.
- 362 Smith, L. N. (2018, mar). A disciplined approach to neural network hyper-
363 parameters: Part 1 – learning rate, batch size, momentum, and weight decay.
- 364 Tolman, H. L. (1991, jun). A Third-Generation Model for Wind Waves on Slowly
365 Varying, Unsteady, and Inhomogeneous Depths and Currents. *J. of Phys.*
366 *Oceanogr.*, *21*(6), 782–797.
- 367 Vannitsem, S., Bremnes, J. B., Demaeyer, J., Evans, G. R., Flowerdew, J., Hemri,
368 S., . . . Ylhaisi, J. (2020, apr). Statistical Postprocessing for Weather Forecasts
369 – Review, Challenges and Avenues in a Big Data World. *arXiv*.
- 370 Veldkamp, S., Whan, K., Dirksen, S., & Schmeits, M. (2020, jul). Statistical post-
371 processing of wind speed forecasts using convolutional neural networks. *arXiv*.
- 372 WAMDI Group, T. (1988). The WAM model - A third generation ocean wave pre-
373 diction model. *Journal of Physical Oceanography*, *18*(12), 1775–1810.
- 374 Wang, S., Cao, J., & Yu, P. S. (2019, jun). *Deep learning for spatio-temporal data*
375 *mining: a survey*. arXiv.
- 376 Weyn, J. A., Durran, D. R., & Caruana, R. (2019, aug). Can Machines Learn to
377 Predict Weather? Using Deep Learning to Predict Gridded 500-hPa Geopotential
378 Height From Historical Weather Data. *Journal of Advances in Modeling*
379 *Earth Systems*, *11*(8), 2680–2693.
- 380 Weyn, J. A., Durran, D. R., & Caruana, R. (2020, mar). Improving data-driven
381 global weather prediction using deep convolutional neural networks on a cubed
382 sphere. *Journal of Advances in Modeling Earth Systems*, *12*(9).
- 383 Wikner, A., Pathak, J., Hunt, B., Girvan, M., Arcomano, T., Szunyogh, I., . . . Ott,
384 E. (2020). Combining machine learning with knowledge-based modeling for
385 scalable forecasting and subgrid-scale closure of large, complex, spatiotemporal
386 systems. *Chaos*, *30*, 53111.
- 387 Yu, F., & Koltun, V. (2015, nov). Multi-Scale Context Aggregation by Dilated Con-
388 volutions. *4th International Conference on Learning Representations, ICLR*
389 *2016 - Conference Track Proceedings*.
- 390 Zjavka, L. (2015, nov). Wind speed forecast correction models using polynomial neu-
391 ral networks. *Renewable Energy*, *83*, 998–1006.